J. Am. Soc. Mass Spectrom. (2015) 26:587–595
DOI: 10.1007/s13361-014-1070-1

FOCUS: EMERGING INVESTIGATORS: RESEARCH ARTICLE

A Comparison of Energy-Resolved Vibrational Activation/Dissociation Characteristics of Protonated and Sodiated High Mannose N-Glycopeptides

Forouzan Aboufazeli, Venkata Kolli, Eric D. Dodds

Department of Chemistry, University of Nebraska-Lincoln, 711 Hamilton Hall, Lincoln, NE 68588-0304, USA

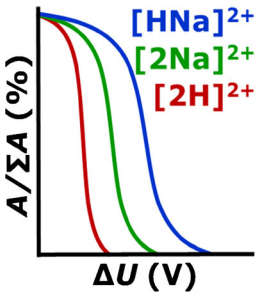

Abstract. Fragmentation of glycopeptides in tandem mass spectrometry (MS/MS) plays a pivotal role in site-specific protein glycosylation profiling by allowing specific oligosaccharide compositions and connectivities to be associated with specific loci on the corresponding protein. Although MS/MS analysis of glycopeptides has been successfully performed using a number of distinct ion dissociation methods, relatively little is known regarding the fragmentation characteristics of glycopeptide ions with various charge carriers. In this study, energy-resolved vibrational activation/dissociation was examined via collision-induced dissociation for a group of related high mannose tryptic glycopeptides as their doubly protonated, doubly sodiated, and hybrid protonated sodium adduct ions. The doubly protonated glycopeptide ions with various compositions were found to undergo fragmentation over a relatively low but wide range of collision energies compared with the doubly sodiated and hybrid charged ions, and were found to yield both glycan and peptide fragmentation depending on the applied collision energy. By contrast, the various doubly sodiated glycopeptides were found to dissociate over a significantly higher but narrow range of collision energies, and exhibited only glycan cleavages. Interestingly, the hybrid protonated sodium adduct ions were consistently the most stable of the precursor ions studied, and provided fragmentation information spanning both the glycan and the peptide moieties. Taken together, these findings illustrate the influence of charge carrier over the energy-resolved vibrational activation/dissociation characteristics of glycopeptides, and serve to suggest potential strategies that exploit the analytically useful features uniquely afforded by specific charge carriers or combinations thereof.

Keywords: *N*-glycopeptides, Tandem mass spectrometry, Collision-induced dissociation

Received: 18 November 2014/Revised: 11 December 2014/Accepted: 16 December 2014/Published Online: 13 January 2015

Introduction

The development of improved capabilities for mass spectrometry (MS) based study of glycoprotein structure is a focal point of activity in bioanalytical science [1–4]. In particular, the analysis of protein glycosylation at the level of proteolytic glycopeptides is of high interest because, unlike methods which involve glycan release, this approach confers protein site specificity to analysis of the modifying glycans [5–8]. While advantageous in allowing for glycans of specific compositions and topologies to be localized to specific sites of a glycoprotein, these means of glycoprotein characterization can also be technically challenging since the heterogeneities and structural complexities of the oligosaccharide and the polypeptide must be addressed simultaneously [9–11]. In this respect, tandem mass spectrometry (MS/MS) methods are of central importance in interrogating the compositions and overall connectivities of glycopeptides [12, 13].

Substantial effort has been directed towards exploiting the specific advantages afforded by different ion dissociation methods for glycopeptide analysis, including those based on ion-neutral interactions, as in collision-induced dissociation (CID) [14–18]; ion-electron and ion-ion reactions, as in electron capture dissociation (ECD) and electron transfer dissociation (ETD) [19–22]; and irradiation with photons, as in infrared multiphoton dissociation (IRMPD) and ultraviolet photodissociation (UVPD) [23–26]. By comparison, less attention has been paid to the effects of charge carrier upon glycopeptide dissociation patterns and energetics. Nevertheless, it has been appreciated that the glycopeptide structural information furnished by a given MS/MS experiment heavily depends on

Correspondence to: Eric D. Dodds; *e-mail:* edodds2@unl.edu

the glycan composition, peptide composition, and ion dissociation method, in addition to the charge state, charge carrier, and the amount of energy deposited to induce fragmentation [27, 28]. Protonated precursor ions are the most common targets for MS/MS analysis of glycopeptides and, as such, the dissociation characteristics of these analytes can in part be rationalized by proton mobility [29, 30]. The study of glycopeptide precursor ions with other charge carriers, which could give rise to fragmentation characteristics that are fundamentally distinct from those of protonated species, may provide some analytical advantages. In this respect, sodiated glycopeptides are of interest, as carbohydrates and glycoconjugates readily appear as alkali metal adducts in MS analysis [31–34], with sodium adducts being the most frequently encountered.

This report presents a study of energy-resolved vibrational activation/dissociation behavior in a group of related high mannose *N*-glycopeptides studied as their $[M + 2H]^{2+}$ (doubly protonated), $[M + 2Na]^{2+}$ (doubly sodiated), and $[M + H + Na]^{2+}$ (hybrid protonated sodium adduct) precursor ions. Glycopeptides of different compositions and with different charge carriers exhibited significantly varied energy-dependent CID characteristics, both in terms of vibrational energy requirements for dissociation, and in terms of the information provided by the resulting fragmentation spectra. These data demonstrate some key respects in which the different charge carriers dictate the energy-resolved vibrational activation/dissociation characteristics of glycopeptides, while also suggesting ways in which analytically useful fragmentation pathways associated with various charge carriers can be exploited for glycopeptide analysis.

Experimental

Materials

Solvents, including HPLC grade water, HPLC grade acetonitrile, and formic acid, were obtained from Burdick and Jackson (Muskegon, MI, USA), Fisher Scientific (Fair Lawn, NJ, USA), and Sigma-Aldrich (St. Louis, MO, USA), respectively. Bovine ribonuclease B (RNase B), urea, sodium acetate, ammonium bicarbonate, dithiothreitol, iodoacetamide, and proteomics grade trypsin were also purchased from Sigma-Aldrich. Zwitterionic hydrophilic interaction liquid chromatography (ZIC HILIC) micropipette tips were acquired from Protea (Somerset, NJ, USA). Corning Pyrex borosilicate melting point capillaries (100 mm×1.5 mm; Corning, NY, USA) were obtained from Fisher Scientific. Platinum wire was acquired from Alfa Aesar (Ward Hill, MA, USA).

Sample Preparation

A solution of 10 $\mu g \cdot \mu L^{-1}$ of RNase B in 8 M urea and 50 mM NH_4HCO_3 (pH 7.5) was prepared to relax the three-dimensional structure of the target protein. A 10 µL aliquot of this denaturing RNase B solution was reduced by addition of 10 µL of 450 mM dithiothreitol in 50 mM NH_4HCO_3 (pH 7.5) and 40 µL of 8 M urea in 50 mM of NH_4HCO_3 (pH 7.5). This mixture was incubated for 1 h in a 55°C water bath. Subsequently, the reduced solution was treated with 10 µL of 500 mM iodoacetamide in 50 mM NH_4HCO_3 (pH 7.5) and incubated in the dark at ambient room temperature for alkylation. The resulting sample was then diluted with 175 µL of 50 mM of NH_4HCO_3 (pH 7.5), followed by addition of 5 µL of 0.5 $\mu g \cdot \mu L^{-1}$ trypsin. The sample was incubated in a 37°C water bath for 16 h for proteolysis. After incubation, the volume of the RNase B trypsin digest was reduced to <10 µL by vacuum centrifugation (Thermo Savant, Holbrook, NY, USA) at ambient room temperature. The total volume of the solution was then increased to 100 µL by adding 80% acetonitrile/0.1% formic acid. Glycopeptides were purified and enriched from the reconstituted crude digest by means of ZIC HILIC micropipette tips. The tip was first washed with water, and then equilibrated with 80% acetonitrile. A 20 µL portion of the reconstituted crude digest was then loaded for purification and enrichment. The tip was next rinsed with 80% acetonitrile, and purified/enriched glycopeptides were eluted in 20 µL of 0.1% formic acid. In some cases, up to 1 mM sodium acetate was spiked into the purified digest in order to increase the proportion of glycopeptide sodium ion adducts for study.

Mass Spectrometry and Tandem Mass Spectrometry

All MS and MS/MS measurements were performed using a Synapt G2-S HDMS quadrupole time-of-flight (Q-TOF) instrument (Waters Corporation; Manchester, UK). For each experiment, 5–10 µL of purified digest was loaded into a homemade borosilicate emitter, which was fabricated from a melting point capillary with the aid of a vertical type micropipette puller (David Kopf Instruments, Tujunga, CA, USA). The filled emitter was then positioned onto the *x*, *y*, *z* stage of the nanoelectrospray ionization (nESI) source. The nESI stage had been adapted to accommodate an electrode holder (Warner Instruments; Holliston, MA, USA) capable of fastening the emitter such that the contained solution was placed into contact with a platinum wire. The nESI capillary potential was delivered to the sample via the platinum wire. All experiments were carried out using nESI capillary voltages ranging between 0.8 and 1.2 kV. The ion source sampling cone voltage and cone offset voltage were optimized in order to obtain the maximum current for each target analyte ion. These settings ranged from 15 to 80 V and from 15 to 50 V, respectively. In general, the optimum intensity of sodium ion adducts was achieved at higher sampling cone voltages than those optimal for observation of protonated ions [32]. All vibrational activation/dissociation experiments were carried out using low-energy transmission type CID. Fragmentation spectra were obtained for quadrupole selected precursor ions using the trapping region stacked ring ion guide of the instrument as the collision cell. Argon served as the collision gas and was admitted to the collision cell to result in a pressure of approximately $5.0 \cdot 10^{-3}$ mbar.

Data Processing and Presentation

All MS and MS/MS spectra were acquired using MassLynx 4.1 (Waters). Data were further processed and visualized using IGOR Pro 6.3 (WaveMetrics, Lake Oswego, OR, USA) and Sigma Plot 10.1 (Systat, Chicago, IL, USA). Glycopeptide fragment ions arising from cleavage of the oligosaccharide moiety were assigned using the nomenclature of Domon and Costello [35], whereas fragments originating from scission of the polypeptide group were named according to the system of Roepstorff and Fohlmann [36]. Occasionally, an observed product ion could have plausibly been formed by more than one specific glycan cleavage; thus, these ambiguous fragments were specified according to the observed monosaccharide loss or losses. Glycan structures were diagrammed using the monosaccharide symbols suggested by Varki et al. [37].

Results

Overview

In order to investigate the influence of different charge carriers on the vibrational activation/dissociation behaviors of model glycopeptides, several N-glycosylated peptides derived from trypsinolysis of RNase B were studied with respect to their energy-resolved CID pathways. Target analyte ions were chosen such that charge state and glycan composition were held constant, while the amino acid composition and combination of charge carriers were varied. All glycopeptide ions studied herein had charge states of $z = 2+$ and carried the $GlcNAc_2Man_5$ high mannose *N*-glycan. Nevertheless, glycopeptides with a diversity of amino acid sequences and compositions were generated by proteolysis owing to the localization of several tryptic cleavage sites near the site of glycosylation. Specifically, glycopeptides with the amino acid sequences NLTK, SRNLTK, NLTKDR, and SRNLTKDR were selected for investigation. In addition, each glycopeptide was studied as the doubly protonated $[M + 2H]^{2+}$ ion, the doubly sodiated $[M + 2Na]^{2+}$ ion, and the hybrid protonated sodium adduct $[M + H + Na]^{2+}$ ion. Glycopeptide ions having each combination of charge carrier and peptide group described above were studied, with one exception. Namely, the glycopeptide ion $[SRNLTKDR + GlcNAc_2Man_5 + 2Na]^{2+}$ was not observed in these experiments. This was not entirely unexpected, as protonation of this highly basic glycopeptide (containing one lysine and two arginine residues) would be predicted to be highly favored compared with sodiation.

Precursor Ion Survival Curves

For each glycopeptide ion of interest, the collision energy (expressed here as the potential difference, ΔU, through which the precursor ions were accelerated prior to ion-neutral collisions) applied for CID was varied in 5 V steps. At each collision energy, the fraction of the integrated peak area attributable to the precursor ion was measured. These precursor ion fractional abundances were plotted as a function of collision energy to yield the precursor ion survival curves presented in Figure 1. Regardless of the charge carrier, the glycopeptide

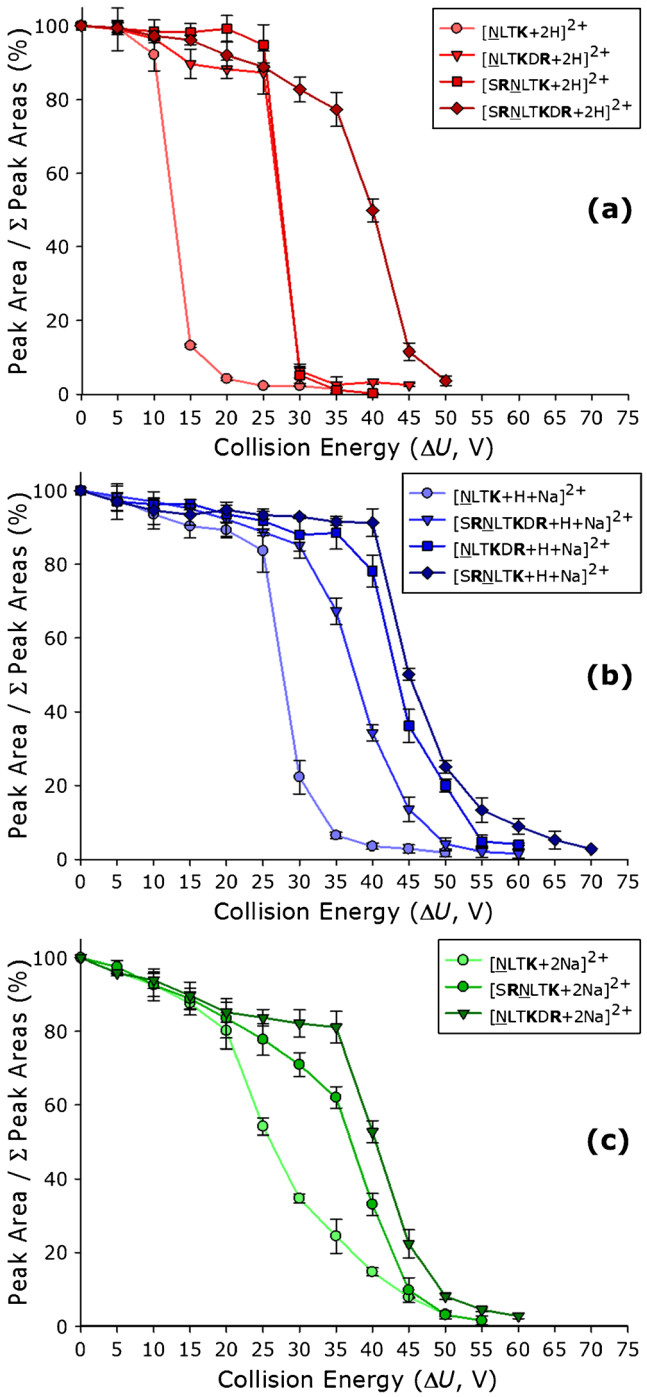

Figure 1. Precursor ion survival curves for the doubly protonated (**a**; red plots), protonated/sodiated hybrid (**b**; blue plots), and doubly sodiated (**c**; green plots) high mannose *N*-glycopeptide ions studied here. The amino acid composition of each glycopeptide is indicated in the corresponding legend, and each glycopeptide harbored the $GlcNAc_2Man_5$ high mannose *N*-glycan. In the legends, basic amino acid residues are bolded, and the glycosylated asparagine residue is underlined. Where visible, error bars represent the standard deviation of three replicate analyses

ions exhibited a range of precursor ion stabilities; however, some interesting trends were noted when comparing precursor ion survivals for doubly protonated, doubly sodiated, and hybrid protonated sodium adduct precursor ions. For example, the collision energy required for depletion of $[M + 2H]^{2+}$ precursor ions to less than 10% of the total integrated peak area ranged from approximately $\Delta U = 20$ V to $\Delta U = 50$ V (Figure 1a). This approximately 30 V range of energies needed to dissociate ≥90% of the initial $[M + 2H]^{2+}$ precursor ion population is similar to that of the $[M + H + Na]^{2+}$ precursor ions. For those protonated sodium adduct hybrid ions, 90% precursor ion depletions were achieved over a range of $\Delta U = 35$ V to $\Delta U = 60$ V, for an approximately 25 V spread (Figure 1b). By contrast, the $[M + 2Na]^{2+}$ precursor ions exhibited a substantially narrower range of 90% precursor ion depletion energies, ranging from approximately $\Delta U = 45$ V to $\Delta U = 50$ V and representing a mere 5 V spread among the precursor ions studied (Figure 1c). Since all of these precursor ions had the same charge state and encompassed a common range of masses (i.e., vibrational degrees of freedom), the differences among their precursor ion survivals point to distinct inherent stabilities and ranges of stabilities among the group of precursor ions depending largely on their charge carriers.

In addition to differing ranges of precursor ion survivals among different charge carriers, differences in the order of precursor stability were also noted among glycopeptide ions with the same charge carrier. Among the precursor ion doubly protonated precursor ions, the order of precursor ion depletion with increasing vibrational energy deposition was consistent with general predictions based on proton mobility [29, 30] as well as predictions for vibrational energy deposition requirement based on the number of vibrational degrees of freedom (Figure 1a) [38, 39]. For instance, the $[NLTK + GlcNAc_2Man_5 + 2H]^{2+}$ underwent dissociation at lower collision energies than the other protonated precursor ions. This observation was in accord with the presence of a readily mobile proton (i.e., the number of charge carrying protons exceeds the number of basic amino acid residues) and the availability of the fewest vibrational modes among the protonated precursors. By contrast, the most stable of the doubly protonated precursors was the $[SRNLTKDR + GlcNAc_2Man_5 + 2H]^{2+}$ precursor ion. This observation was consistent with the lack of a readily mobile proton (i.e., the number of basic amino acid residues exceeds the number of charge carrying protons) and the greatest number of available normal modes for this analyte compared with the other protonated precursors.

Interestingly, such arguments were not always able to predict the order of stability among the hybrid charged $[M + H + Na]^{2+}$ precursor ions. The glycopeptides NLTK + $GlcNAc_2Man_5$, NLTKDR + $GlcNAc_2Man_5$, and SRNLTK + $GlcNAc_2Man_5$ each exhibited an increase in stability as their hybrid charged forms in comparison to their solely protonated forms. This can be viewed as consistent with expectations based on proton mobility, as the transition from $[M + 2H]^{2+}$ to $[M + H + Na]^{2+}$ brings the amino acid NLTK from harboring a readily mobile proton to only a partially mobile proton; meanwhile, the amino acid compositions NLTKDR and SRNLTK shift from harboring a partially mobile proton to no mobile protons [40]. By contrast, the glycopeptide SRNLTKDR + $GlcNAc_2Man_5$ was found to have very similar precursor ion survival characteristics both as the $[M + 2H]^{2+}$ ion and the $[M + H + Na]^{2+}$ ion. With either combination of charge carriers, this glycopeptide did not contain a mobile proton; therefore, a significant shift in precursor ion survival might not be expected. The end result of this was that the more massive $[SRNLTKDR + GlcNAc_2Man_5 + H + Na]^{2+}$ ion fragmented more readily than the $[NLTKDR + GlcNAc_2Man_5 + H + Na]^{2+}$ and $[SRNLTK + GlcNAc_2Man_5 + H + Na]^{2+}$ precursors (Figure 1b). This occurred despite the lack of a readily mobile proton in any of these three glycopeptide ions, and despite the greater vibrational energy capacity of the larger but evidently less stable ion. Finally, Figure 1c demonstrates that the $[M + 2Na]^{2+}$ ions exhibit a similar trend to that of the hybrid ionic form, although as noted above we were not able to observe the $[SRNLTKDR + GlcNAc_2Man_5 + 2Na]^{2+}$. Nevertheless, each glycopeptide ion studied here was found to be most stable as the hybrid $[M + H + Na]^{2+}$ ion compared with the $[M + 2H]^{2+}$ and $[M + 2Na]^{2+}$ precursor ions.

In order to more quantitatively assess differences in stability among the various precursor ions, precursor ion kinetic energies, which brought about 50% precursor ion survival, were calculated. The kinetic energy E_k of a precursor ion accelerated through a potential difference ΔU is given by:

$$E_k = ze\Delta U \tag{1}$$

where z is the integer charge and e is the fundamental charge. The precursor ion kinetic energy E_{k50}, which results in 50% precursor ion survival, thus relates to the corresponding potential difference ΔU_{50} according to:

$$E_{k50} = ze\Delta U_{50} \tag{2}$$

Here, values of ΔU_{50} were determined by fitting the linear portions of the precursor ion survival curves. The value of E_{k50} alone is of limited use for comparing precursor ion stabilities, as the amount of vibrational energy required to bring about unimolecular dissociation also depends on the number of available vibrational degrees of freedom, f_v [38, 39]. The value of f_v is calculated as:

$$f_v = 3n - 6 \tag{3}$$

for an analyte comprised of n atoms. Given these values, it is possible to calculate a vibrational degrees of freedom

normalized precursor ion kinetic energy, which corresponds to 50% precursor ion survival, E_{n50}:

$$E_{n50} = \frac{10^2 z \Delta U_{50}}{f_v} \quad (4)$$

In Equation (4), the factor of 10^2 was added merely to provide more convenient figures for comparison. The E_{n50} values for the various glycopeptides studied here are reported in Table 1. These data demonstrate that the range of E_{n50} values range more widely for the $[M + 2H]^{2+}$ precursor ions (3.69–8.78, for a range of 5.09) than for the $[M + H + Na]^{2+}$ precursor ions (11.7–8.20, for a range of 3.50) or the $[M + 2Na]^{2+}$ precursor ions (7.82–10.1, for a range of 2.28). These results also highlight that the combination of charge carriers that results in the most stable precursor ions is the hybrid $[M + H + Na]^{2+}$ precursor ion. Although the explanation for enhanced stability of the $[M + H + Na]^{2+}$ ions is not entirely clear at present, we speculate that charge carrier localization may be partially responsible. Previous work of Lebrilla and coworkers suggested that in high-mannose *N*-glycopeptides, sodiation primarily occurs on the glycan moiety [27]. In the hybrid protonated sodium adducts, protonation most likely occurs on the peptide group, whereas the sodium ion is most likely bound to the glycan. This is in contrast to the doubly sodiated precursor ions, in which the presence of two sodium ions on the glycan may lead to a coulombically less stable arrangement of charge carriers. Interestingly, CID spectra of the doubly sodiated glycopeptide ions provided no evidence for cation localization at the peptide (as discussed in the succeeding section), which may be consistent with this notion.

These general observations are reiterated in Figure 2, which presents the precursor ion survival curves of SRNLTK + $GlcNAc_2Man_5$ and NLTKDR + $GlcNAc_2Man_5$ as their $[M + 2H]^{2+}$, $[M + H + Na]^{2+}$, and $[M + 2Na]^{2+}$ precursor ions. Both data sets demonstrate similar energy-resolved disappearance behaviors among glycopeptide ions having different compositions but the same charge carriers; however, glycopeptide ions of a given glycopeptide composition demonstrated markedly different precursor ion survivals for each of the different manners of carrying charge. The precursor ion survival curves

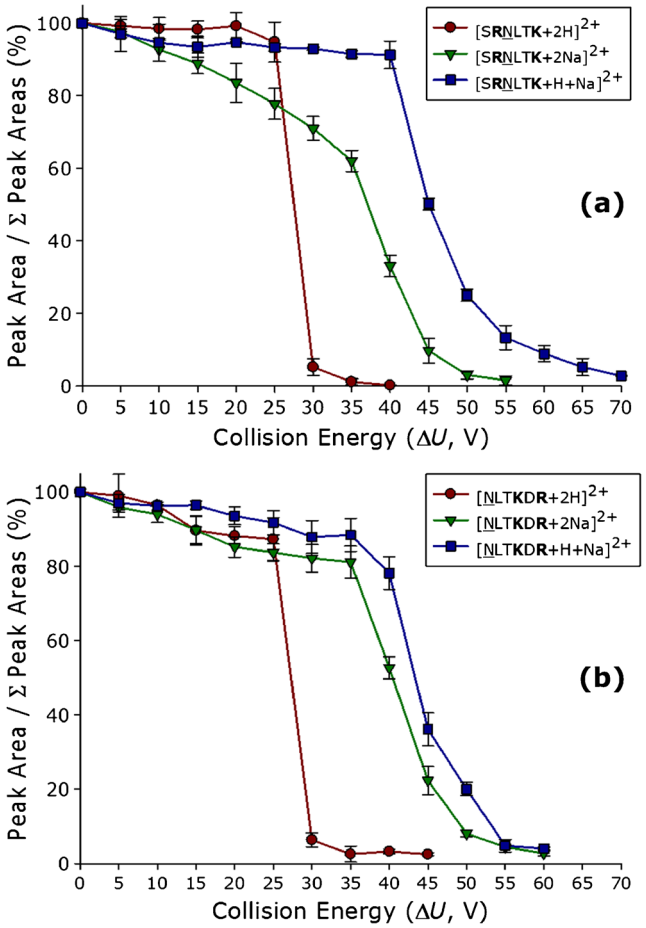

Figure 2. Precursor ion survival curves for SRNLTK + $GlcNAc_2Man_5$ (**a**) and NLTKDR + $GlcNAc_2Man_5$ (**b**) as their doubly protonated (red plots), protonated/sodiated hybrid (blue plots), and doubly sodiated (green plots) precursor ions. In the legends, basic amino acid residues are bolded, and the glycosylated asparagine residue is underlined. Where visible, error bars represent the standard deviation of three replicate analyses

Table 1. Vibrational Activation/Dissociation Collision Energies Resulting in 50% Precursor Ion Survival of the High Mannose *N*-Glycopeptide Ions Studied Here

Glycopeptide composition	Charge carrier	z	f_v	ΔU_{50} (V)	$E_{n\ 50}$
NLT**K** + $GlcNAc_2Man_5$	$[M + 2H]^{2+}$	2	693	12.8	3.69
	$[M + H + Na]^{2+}$			28.4	8.20
	$[M + 2Na]^{2+}$			27.1	7.82
SR**N**LT**K** + $GlcNAc_2Man_5$	$[M + 2H]^{2+}$	2	801	27.5	6.87
	$[M + H + Na]^{2+}$			46.7	11.7
	$[M + 2Na]^{2+}$			37.1	9.26
NLT**KDR** + $GlcNAc_2Man_5$	$[M + 2H]^{2+}$	2	807	27.3	6.77
	$[M + H + Na]^{2+}$			44.3	11.0
	$[M + 2Na]^{2+}$			40.7	10.1
SR**N**LT**KDR** + $GlcNAc_2Man_5$	$[M + 2H]^{2+}$	2	897	39.4	8.78
	$[M + H + Na]^{2+}$			37.5	9.36

The ΔU_{50} values obtained from precursor ion survival curves were normalized for precursor ion charge state (z) and the vibrational degrees of freedom of the neutral glycopeptide (f_v) calculated according to Equation (3). The resulting E_{n50} values were calculated according to Equation (4). Within the glycopeptide compositions, basic amino acid residues are bolded, and the glycosylated asparagine residue is underlined

shown in Figures 2a and b are directly comparable in that the two analytes have nearly the same number of vibrational degrees of freedom (f_v=801 for SRNLTK + $GlcNAc_2Man_5$; f_v=807 for NLTKDR + $GlcNAc_2Man_5$) and, as all of the precursor ions studied here, have the same charge state (z=2). Their overall compositions are also quite similar, involving only the substitution of a serine residue for an aspartic acid residue. Despite these similarities and the qualitative characteristics common to the precursor ion survival curves of the two glycopeptides as variously charged ions, there were some important, albeit subtle, differences to note. For instance, although the monosaccharide compositions of the two glycopeptides are identical and the amino acid compositions are very similar, the sequence of amino acids positions the two basic amino acid residues of each glycopeptide quite differently relative to each other; moreover, an acidic amino acid residue is present in one glycopeptide but not in the other. These features suggest the possibility for significant differences in the manner of charge localization and charge solvation (e.g., proton bridging) between the two glycopeptides. Such distinctions might explain the noticeably greater stability of the $[NLTKDR + GlcNAc_2Man_5 + 2Na]^{2+}$ ion compared with the $[SRNLTK + GlcNAc_2Man_5 + 2Na]^{2+}$ ion (cf., Table 1 and Figure 2a, b).

Vibrational Activation/Dissociation Spectra

Detailed fragmentation maps of the SRNLTK + $GlcNAc_2Man_5$ and NLTKDR + $GlcNAc_2Man_5$ glycopeptides have been diagrammed in Figure 3. Although other fragment ions are formally possible, they have not been indicated in the figure for the sake of simplicity. Likewise, not all potential fragment ions shown in the diagrams were observed within any single CID spectrum. However, these fragmentation maps do provide a quick reference key to various fragment ion types discussed below.

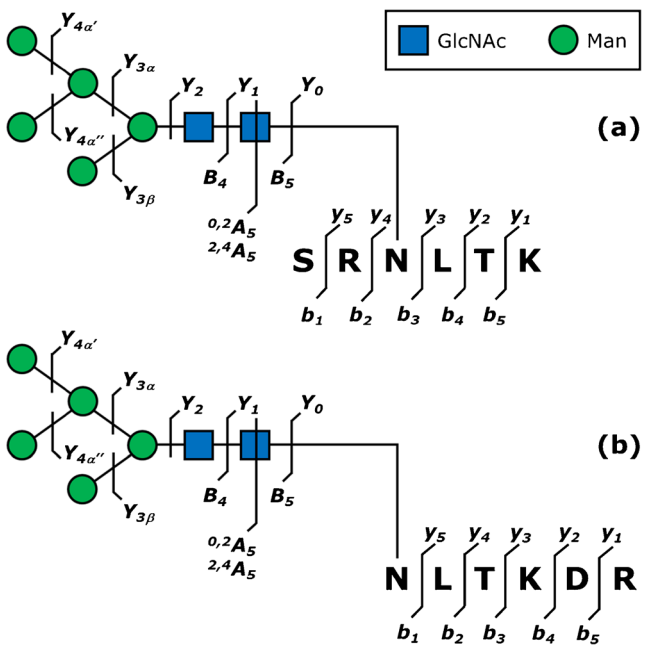

Figure 3. Maps of selected potential glycan and peptide cleavage types for SRNLTK + $GlcNAc_2Man_5$ (**a**) and NLTKDR + $GlcNAc_2Man_5$ (**b**). A key to the relevant monosaccharide symbols is provided in the legend. Abbreviations are used for mannose (Man) and *N*-acetylglucosamine (GlcNAc)

CID spectra of SRNLTK + $GlcNAc_2Man_5$ are shown for the $[M + 2H]^{2+}$, $[M + H + Na]^{2+}$, and $[M + 2Na]^{2+}$ precursor ions in Figure 4. The applied collision energies for the spectra shown in Figure 4a–c were chosen such that approximately 5%–15% of the precursor ion remained (i.e., the precursor ion had been sufficiently activated to deplete most of the population). In accord with the discussion above, this required the application of different collision energies depending on the charge carrier: the $[M + 2H]^{2+}$, $[M + H + Na]^{2+}$, and $[M + 2Na]^{2+}$ precursor ions were subjected to ΔU = 30.0 V, ΔU = 60.0 V, and ΔU = 45.0 V, respectively. Importantly, at 5%–15% precursor ion survival, the three precursor ions yielded quite different dissociation spectra. For instance, the doubly protonated precursor ion yielded a prominent series of *Y* type mannose loss fragments arising from cleavage of the carbohydrate moiety (Figure 4a). Members of this series were observed in both singly charged and doubly charged states. The Y_1 glycan fragment (i.e., the peptide group with one remaining GlcNAc residue attached) was also observed, and by a significant margin constituted the most abundant fragment ion in this spectrum. This is consistent with previous observations that cleavage between the two GlcNAc residues of the *N*-linked glycan core is a favored process [14–18]. Under these conditions, the CID spectrum of the hybrid protonated sodium adduct (Figure 4b) was highly distinct from that of the doubly protonated precursor. In this spectrum, the major fragments arose as a result of *B* type cleavage of the glycan moiety, most abundantly producing the B_4 ion (the fragment complementary to the Y_1 fragment mentioned previously), which arises from cleavage of the GlcNAc-GlcNAc glycosidic linkage. Also dissimilar from the doubly protonated glycopeptide, this precursor ion further furnished multiple peptide backbone fragmentations (involving b_2, b_5, and y_2 cleavages) as well as cross-ring cleavages of the reducing terminal GlcNAc (corresponding to $^{2,4}A_5$ and $^{0,2}A_5$ fragmentations). Consistent with previous experimental and theoretical findings, the peptide backbone fragments carried the proton as the charge carrier, while the glycan fragments retained the sodium ion [27]. In general, the CID spectrum of the doubly sodiated ion at 5%–15% precursor survival (Figure 4c) resembled that of the hybrid protonated sodium adduct more so than the doubly protonated precursor ion in general appearance and types of fragmentation; however, the doubly sodium coordinated glycopeptide provided a less informative spectrum with generally fewer fragment ions and lacking any detectable peptide sequence ions. Nevertheless, these ions still produced cross-ring cleavages ($^{0,2}A_5$ and $^{2,4}A_5$ product ions), which can be useful in distinguishing between free glycans and glycoconjugates [41]. Overall, the CID spectra of the doubly sodiated glycopeptide revealed no peptide fragments. In contrast, the doubly protonated and hybrid ionic forms produced both carbohydrate and some peptide fragmentation.

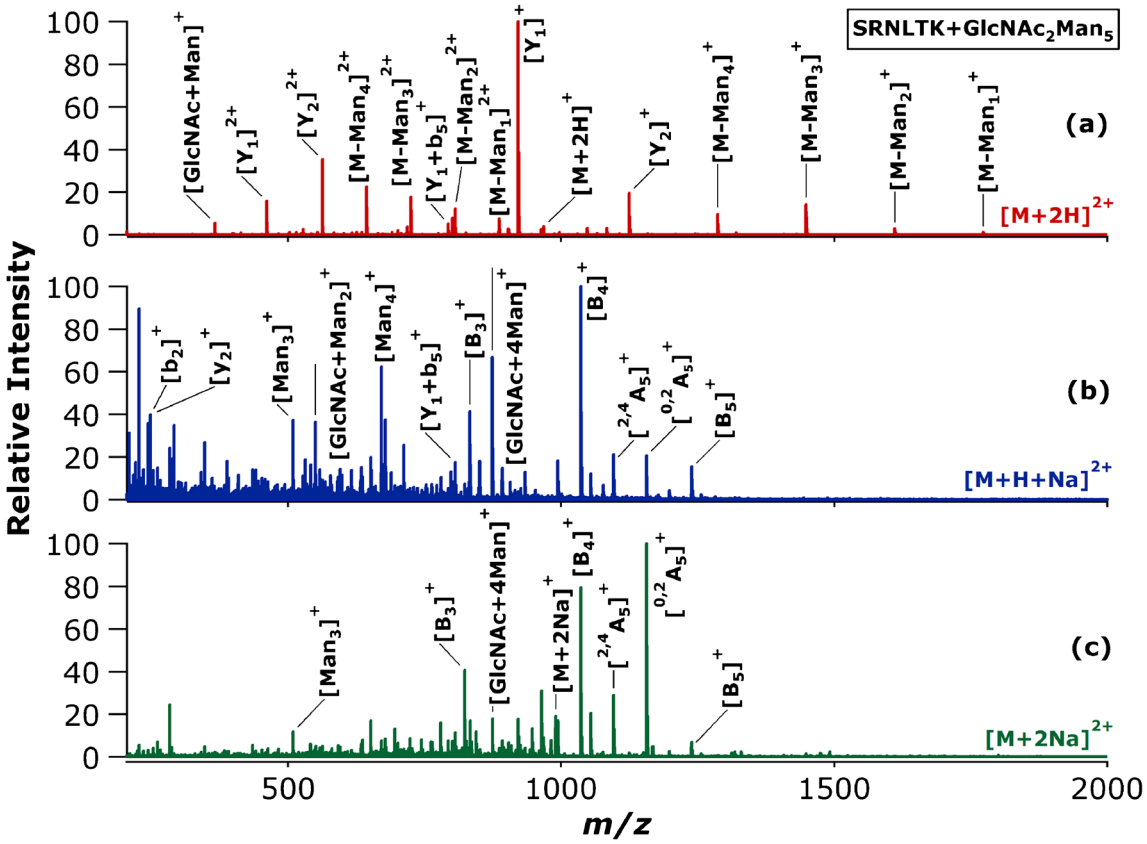

Figure 4. Vibrational activation/dissociation spectra for the SRNLTK + $GlcNAc_2Man_5$ glycopeptide as the doubly protonated (**a**; red trace), protonated/sodiated hybrid (**b**; blue trace), and doubly sodiated (**c**; green trace) precursor ion. Each spectrum was acquired at a collision energy that resulted in approximately 5%–15% precursor ion survival: ΔU=30.0 V (**a**); ΔU=60.0 V (**b**); and ΔU=45.0 V (**c**)

In addition, the carbohydrate cleavages that were not accessible in the doubly protonated glycopeptide fragmentation were detected in the sodium adduct ions (e.g., cross-ring cleavages).

To further explore differences and similarities among the fragmentation behaviors of the variously charged precursor ions, the $[M + 2H]^{2+}$, $[M + H + Na]^{2+}$, and $[M + 2Na]^{2+}$ precursor ions of the NLTKDR + $GlcNAc_2Man_5$ glycopeptide were studied at a fixed collision energy of ΔU = 35.0 V (Figure 5). This specific collision energy was chosen because it lies approximately half-way between the ΔU_{50} values of the $[NLTKDR + GlcNAc_2Man_5 + 2H]^{2+}$ and the $[NLTKDR + GlcNAc_2Man_5 + H + Na]^{2+}$ precursor ions (cf. Table 1). The comparison shown in Figure 5, therefore, is in contrast to the collision energies applied in Figure 4, which were varied in order to achieve a given level of precursor ion depletion. At this fixed collision energy, doubly protonated NLTKDR + $GlcNAc_2Man_5$ glycopeptide ions readily lost mannose residues, yielding an assortment of *Y* fragments (Figure 5a). Under these conditions, the peptide backbone remained intact, whereas the major fragmentation product corresponded to the Y_1 ion (i.e., peptide chain plus reducing terminal GlcNAc residue). At the same collision energy, the doubly sodiated and hybrid protonated sodium adduct forms were found to undergo entirely different patterns of dissociation compared with the doubly protonated precursor (Figure 5b, c). For instance, the $[M + 2Na]^{2+}$ precursor ion yielded *A*, *B*, and *Y* type fragments (Figure 5c). The $[M + H + Na]^{2+}$ precursor ion exhibited a combination of general characteristics shared with doubly sodiated and doubly protonated glycopeptides resulting in *A*, *B*, *Y* type glycan cleavages, in addition to peptide cleavage products involving loss of the C-terminal arginine residue (Figure 5b). This cleavage C-terminal to the aspartic acid residue in the absence of a readily mobile proton is consistent with the aspartic acid effect [42], and loss of the protonated arginine fragment in a y_1 type cleavage is consistent with the greater gas-phase basicity of arginine compared with lysine [43]. Overall, this comparison in the fragmentation of NLTKDR + $GlcNAc_2Man_5$ as $[M + 2H]^{2+}$, $[M + H + Na]^{2+}$, and $[M + 2Na]^{2+}$ precursor ions underscores that at constant collision energy, precursor ions of nearly the same *m/z* will undergo fragmentation through significantly different channels depending upon the identity of the charge carriers. This has significant implications for the automated acquisition of CID spectra (for example, during an LC-MS/MS experiment), since often the collision energy is set based solely on *m/z* [44]. For these precursor ions, such a strategy would lead to the acquisition of MS/MS spectra with entirely different information content and would, accordingly, necessitate different approaches to interpretation.

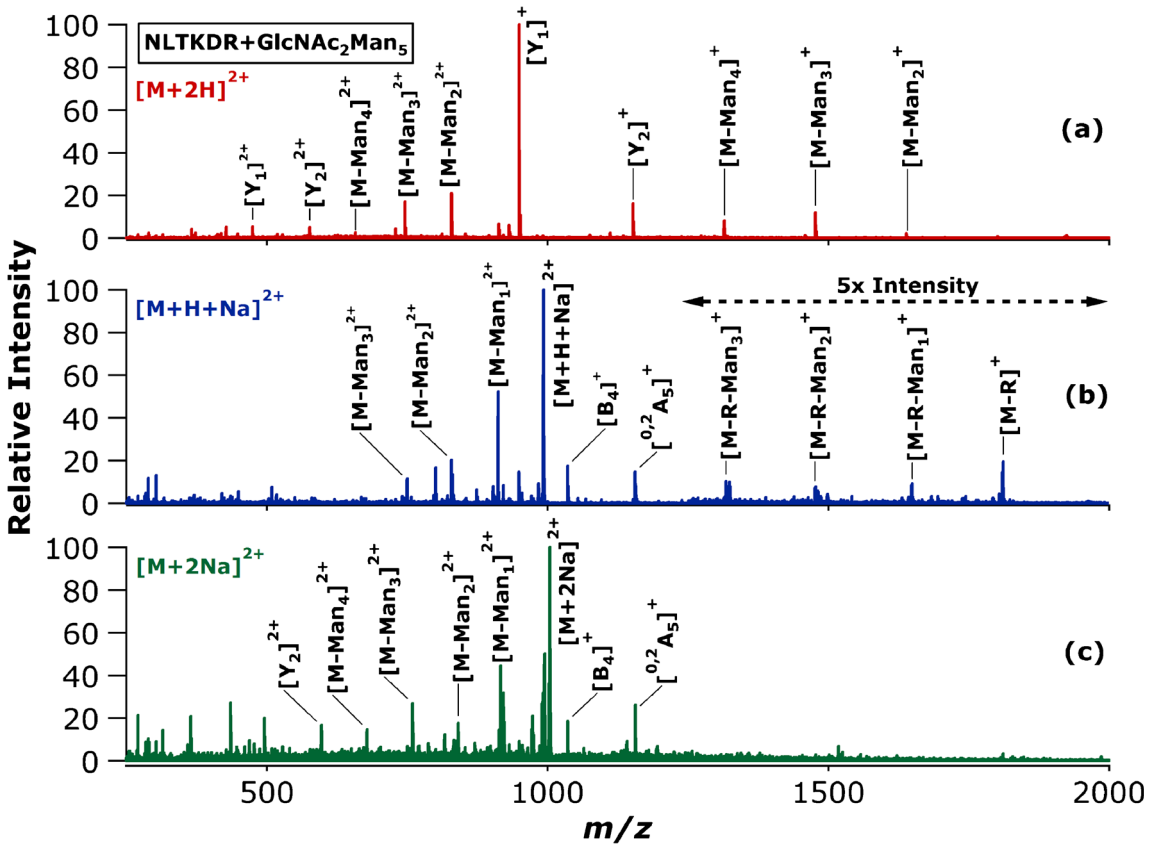

Figure 5. Vibrational activation/dissociation spectra for the NLTKDR + $GlcNAc_2Man_5$ glycopeptide as the doubly protonated (**a**; red trace), protonated/sodiated hybrid (**b**; blue trace), and doubly sodiated (**c**; green trace) precursor ion. Each spectrum was acquired at the same collision energy of ΔU=35

Conclusions

Here, the energy-resolved vibrational activation/dissociation of model glycopeptides charged as $[M + 2H]^{2+}$, $[M + H + Na]^{2+}$, and $[M + 2Na]^{2+}$ precursor ions has been systematically compared. In general, the 50% precursor ion survivals of doubly protonated precursor ions varied the most widely, with hybrid protonated sodium adducts and doubly sodiated ions exhibiting 50% precursor ion survivals that were less sensitive to the precursor ion composition and vibrational degrees of freedom. In addition, the hybrid charged $[M + H + Na]^{2+}$ ions required consistently greater vibrational energy deposition in order to achieve fragmentation compared with either the $[M + 2H]^{2+}$ or $[M + 2Na]^{2+}$ ions. While the glycopeptide ions with various combinations of charge carriers were found to have different inherent stabilities, the product ions yielded by the various precursor ions also varied substantially. Overall, the doubly protonated precursor ions showed potential to provide fragmentation information on both the oligosaccharide (*Y* type cleavages) and, at higher collision energies, the polypeptide (*b* and *y* type cleavages) moieties. By contrast, dissociation of the doubly sodiated precursor ions was primarily characterized by glycan cleavage (*A* and *B* type ions) with loss of the peptide group, leading to no amino acid sequence information. Interestingly, the hybrid charged protonated sodium adducts of glycopeptides provided some of the favorable fragmentation characteristics of both the doubly protonated and doubly sodiated precursor ions, making this type of precursor ion an interesting target for future study. Finally, these results suggest that the selection of charge carriers for glycopeptide MS/MS analysis by CID involves a compromise between charge carriers that provide the most extensive structural information, yet result in wide-ranging precursor ion stabilities (i.e., $[M + 2H]^{2+}$ ions), and charge carriers that result in precursor ions with similar energetic requirements for dissociation but less information on the overall connectivity of the glycopeptide (i.e., $[M + 2Na]^{2+}$). These observations are of significant practical relevance from the standpoints of charge carrier selection, collision energy selection, and MS/MS spectral interpretation for glycosylated peptide ions.

Acknowledgments

The authors gratefully acknowledge funding from the University of Nebraska, which was provided in part by the Nebraska Tobacco Settlement Biomedical Research Development Fund The authors also thank Katherine N. Schumacher and Abby S. Gelb for critical readings of the manuscript.

References

1. Morelle, W., Canis, K., Chirat, F., Faid, V., Michalski, J.C.: The use of mass spectrometry for the proteomic analysis of glycosylation. Proteomics **6**, 3993–4015 (2006)
2. Marino, K., Bones, J., Kattla, J.J., Rudd, P.M.: A systematic approach to protein glycosylation analysis: a path through the maze. Nat. Chem. Biol. **6**, 713–723 (2010)
3. Schiel, J.E.: Glycoprotein analysis using mass spectrometry: unraveling the layers of complexity. Anal. Bioanal. Chem. **404**, 1141–1149 (2012)
4. Alley, W.R., Mann, B.F., Novotny, M.V.: High-sensitivity analytical approaches for the structural characterization of glycoproteins. Chem. Rev. **113**, 2668–2732 (2013)
5. Dalpathado, D.S., Desaire, H.: Glycopeptide analysis by mass spectrometry. Analyst **133**, 731–738 (2008)
6. An, H.J., Froehlich, J.W., Lebrilla, C.B.: Determination of glycosylation sites and site-specific heterogeneity in glycoproteins. Curr. Opin. Chem. Biol. **13**, 421–426 (2009)
7. Tissot, B., North, S.J., Ceroni, A., Pang, P.-C., Panico, M., Rosati, F., Capone, A., Haslam, S.M., Dell, A., Morris, H.R.: Glycoproteomics: past, present, and future. FEBS Lett. **583**, 1728–1735 (2009)
8. Desaire, H.: Glycopeptide analysis, recent developments and applications. Mol. Cell. Proteom. **12**, 893–901 (2013)
9. Clowers, B.H., Dodds, E.D., Seipert, R.R., Lebrilla, C.B.: Site determination of protein glycosylation based on digestion with immobilized nonspecific proteases and Fourier transform ion cyclotron resonance mass spectrometry. J. Proteome Res. **6**, 4032–4040 (2007)
10. Dodds, E.D., Seipert, R.R., Clowers, B.H., German, J.B., Lebrilla, C.B.: Analytical performance of immobilized pronase for glycopeptide footprinting and implications for surpassing reductionist glycoproteomics. J. Proteome. Res. **8**, 502–512 (2009)
11. Froehlich, J.W., Dodds, E.D., Wilhelm, M., Serang, O., Steen, J.A., Lee, R.S.: A classifier based on accurate mass measurements to aid large scale, unbiased glycoproteomics. Mol. Cell. Proteom. **12**, 1017–1025 (2013)
12. Wuhrer, M., Catalina, M.I., Deelder, A.M., Hokke, C.H.: Glycoproteomics based on tandem mass spectrometry of glycopeptides. J. Chromatogr. B. **849**, 115–128 (2007)
13. Dodds, E.D.: Gas-phase dissociation of glycosylated peptide ions. Mass Spectrom. Rev. **31**, 666–682 (2012)
14. Segu, Z.M., Mechref, Y.: Characterizing protein glycosylation sites through higher-energy C-trap dissociation. Rapid Commun. Mass Spectrom. **24**, 1217–1225 (2010)
15. Hart-Smith, G., Raftery, M.J.: Detection and characterization of low abundance glycopeptides via higher-energy c-trap dissociation and orbitrap mass analysis. J. Am. Soc. Mass Spectrom. **23**, 124–140 (2012)
16. Vekey, K., Ozohanics, O., Toth, E., Jeko, A., Revesz, A., Krenyacz, J., Drahos, L.: Fragmentation characteristics of glycopeptides. Int. J. Mass Spectrom. **345/347**, 71–79 (2013)
17. Cao, Q., Zhao, X., Zhao, Q., Lv, X., Ma, C., Li, X., Zhao, Y., Peng, B., Ying, W., Qian, X.: Strategy integrating stepped fragmentation and glycan diagnostic ion-based spectrum refinement for the identification of core fucosylated glycoproteome using mass spectrometry. Anal. Chem. **86**, 6804–6811 (2014)
18. Kolli, V., Dodds, E.D.: Energy-resolved collision-induced dissociation pathways of model N-linked glycopeptides: implications for capturing glycan connectivity and peptide sequence in a single experiment. Analyst **139**, 2144–2153 (2014)
19. Alley, W.R., Mechref, Y., Novotny, M.V.: Characterization of glycopeptides by combining collision-induced dissociation and electron-transfer dissociation mass spectrometry data. Rapid Commun. Mass Spectrom. **23**, 161–170 (2009)
20. Chalkley, R.J., Thalhammer, A., Schoepfer, R., Burlingame, A.L.: Identification of protein O-GlcN acylation sites using electron transfer dissociation mass spectrometry on native peptides. Proc. Natl. Acad. Sci. U. S. A. **106**, 8894–8899 (2009)
21. Singh, C., Zampronio, C.G., Creese, A.J., Cooper, H.J.: Higher energy collision dissociation (HCD) product ion-triggered electron transfer dissociation (ETD) mass spectrometry for the analysis of N-linked glycoproteins. J. Proteome Res. **11**, 4517–4525 (2012)
22. Manri, N., Satake, H., Kaneko, A., Hirabayashi, A., Baba, T., Sakamoto, T.: Glycopeptide identification using liquid-chromatography-compatible hot electron capture dissociation in a radio-frequency-quadrupole ion trap. Anal. Chem. **85**, 2056–2063 (2013)
23. Adamson, J.T., Hakansson, K.: Infrared multiphoton dissociation and electron capture dissociation of high-mannose type glycopeptides. J. Proteome. Res. **5**, 493–501 (2006)
24. Bindila, L., Steiner, K., Schaffer, C., Messner, P., Mormann, M., Peter-Katalinic, J.: Sequencing of *O*-glycopeptides derived from an S-layer glycoprotein of *Geobacillus stearothermophilus* NRS 2004/3a containing up to 51 monosaccharide residues at a single glycosylation site by Fourier transform ion cyclotron resonance infrared multiphoton dissociation mass spectrometry. Anal. Chem. **79**, 3271–3279 (2007)
25. Zhang, L., Reilly, J.P.: Extracting both peptide sequence and glycan structural information by 157 nm photodissociation of N-linked glycopeptides. J. Proteome. Res. **8**, 734–742 (2008)
26. Madsen, J.A., Ko, B.J., Xu, H., Iwashkiw, J.A., Robotham, S.A., Shaw, J.B., Feldman, M.F., Brodbelt, J.S.: Concurrent automated sequencing of the glycan and peptide portions of O-linked glycopeptide anions by ultraviolet photodissociation mass spectrometry. Anal. Chem. **85**, 9253–9261 (2013)
27. Seipert, R.R., Dodds, E.D., Clowers, B.H., Beecroft, S.M., German, J.B., Lebrilla, C.B.: Factors that influence fragmentation behavior of N-linked glycopeptide ions. Anal. Chem. **80**, 3684–3692 (2008)
28. Seipert, R.R., Dodds, E.D., Lebrilla, C.B.: Exploiting differential dissociation chemistries of O-linked glycopeptide ions for the localization of mucin-type protein glycosylation. J. Proteome. Res. **8**, 493–501 (2009)
29. Dongre, A.R., Jones, J.L., Somogyi, A., Wysocki, V.H.: Influence of peptide composition, gas-phase basicity, and chemical modification on fragmentation efficiency: evidence for the mobile proton model. J. Am. Chem. Soc. **118**, 8365–8374 (1996)
30. Wysocki, V.H., Tsaprailis, G., Smith, L.L., Breci, L.A.: Mobile and localized protons: a framework for understanding peptide dissociation. J. Mass Spectrom. **35**, 1399–1406 (2000)
31. Cancilla, M.T., Penn, S.G., Carroll, J.A., Lebrilla, C.B.: Coordination of alkali metals to oligosaccharides dictates fragmentation behavior in matrix assisted laser desorption ionization/Fourier transform mass spectrometry. J. Am. Chem. Soc. **118**, 6736–6745 (1996)
32. Clowers, B.H., Dodds, E.D., Seipert, R.R., Lebrilla, C.B.: Dual polarity accurate mass calibration for electrospray ionization and matrix-assisted laser desorption/ionization mass spectrometry using maltooligosaccharides. Anal. Biochem. **381**, 205–213 (2008)
33. Jiang, W., Wysocki, V.H., Dodds, E.D., Miesfeld, R.L., Scaraffia, P.Y.: Differentiation and quantification of C1 and C2 C-13-labeled glucose by tandem mass spectrometry. Anal. Biochem. **404**, 40–44 (2010)
34. Huang, Y., Dodds, E.D.: Ion mobility studies of carbohydrates as group I adducts: isomer specific collisional cross section dependence on metal ion radius. Anal. Chem. **85**, 9728–9735 (2013)
35. Domon, B., Costello, C.E.: A systematic nomenclature for carbohydrate fragmentations in FAB-MS/MS spectra of glycoconjugates. Glycoconj. J. **5**, 397–409 (1988)
36. Roepstorff, P., Fohlmann, J.: Proposal for a common nomenclature for sequence ions in mass spectra of peptides. Biomed. Mass Spectrom. **11**, 601 (1984)
37. Varki, A., Cummings, R.D., Esko, J.D., Freeze, H.H., Stanley, P., Marth, J.D., Bertozzi, C.R., Hart, G.W., Etzler, M.E.: Symbol nomenclature for glycan representation. Proteomics **9**, 5398–5399 (2009)
38. Memboeuf, A., Nasioudis, A., Indelicato, S., Pollreisz, F., Kuki, A.K., Kéki, S.N., van den Brink, O.F., Vékey, K.R., Drahos, L.S.: Size effect on fragmentation in tandem mass spectrometry. Anal. Chem. **82**, 2294–2302 (2010)
39. Indelicato, S., Bongiorno, D., Indelicato, S., Drahos, L., Turco Liveri, V., Turiák, L., Vékey, K., Ceraulo, L.: Degrees of freedom effect on fragmentation in tandem mass spectrometry of singly charged supramolecular aggregates of sodium sulfonates. J. Mass Spectrom. **48**, 379–383 (2013)
40. Kapp, E.A., Schütz, F., Reid, G.E., Eddes, J.S., Moritz, R.L., O'Hair, R.A.J., Speed, T.P., Simpson, R.J.: Mining a tandem mass spectrometry database to determine the trends and global factors influencing peptide fragmentation. Anal. Chem. **75**, 6251–6264 (2003)
41. Vakhrushev, S.Y., Zamfir, A., Peter-Katalinić, J.: 0.2An cross-ring cleavage as a general diagnostic tool for glycan assignment in glycoconjugate mixtures. J. Am. Soc. Mass Spectrom. **15**, 1863–1868 (2004)
42. Paizs, B., Suhai, S.: Fragmentation pathways of protonated peptides. Mass Spectrom. Rev. **24**, 508–548 (2005)
43. Harrison, A.G.: The gas-phase basicities and proton affinities of amino acids and peptides. Mass Spectrom. Rev. **16**, 201–217 (1997)
44. Froehlich, J.W., Barboza, M., Chu, C., Lerno, L.A., Clowers, B.H., Zivkovic, A.M., German, J.B., Lebrilla, C.B.: Nano-LC-MS/MS of glycopeptides produced by nonspecific proteolysis enables rapid and extensive site-specific glycosylation determination. Anal. Chem. **83**, 5541–5547 (2011)